7-7-2015

Enhanced Rates of Photoinduced Molecular Orientation in a Series of Molecular Glassy Thin Films.

Kristen E Snell

Renjie Hou

Eléna Ishow

François Lagugné-Labarthet

Enhanced Rates of Photoinduced Molecular Orientation in a Series of Molecular Glassy Thin Films

*Kristen E. Snell,[†,‡] Renjie Hou, [‡] Eléna Ishow,[†] François Lagugné-Labarthet[‡]**

[†] CEISAM–UMR CNRS 6230, Université de Nantes, 2 rue de la Houssinière, 44322 Nantes, France. [‡] Departments of Chemistry and Physics & Astronomy, University of Western Ontario, 1151 Richmond street, London, ON, Canada, N6A5B7.

KEYWORDS. Molecular glass, Azo thin films, Polarization modulation infrared spectroscopy, Birefringence, Photoinduced anisotropy, Photoisomerization.

ABSTRACT: Photoinduced orientation in a series of molecular glasses made of small push-pull azo derivatives is dynamically investigated for the first time. Birefringence measurements at 632.8 nm are conducted with a temporal resolution of 100 ms in order to probe the fast rate of the azo orientation induced under polarized light and its temporal stability over several consecutive cycles. In order to better evaluate the influence of the azo chemical substituents and their electronic properties on the orientation of the whole molecule, a series of push-pull azo derivatives involving a triphenylaminoazo core substituted with distinct electron-withdrawing moieties is studied. All resulting thin films are probed using polarization modulation infrared spectroscopy that yields dynamical linear dichroism measurements during a cycle of orientation followed by relaxation. We show here in particular that the orientation rates of small molecule-based azo materials are systematically increased up to a 7-fold factor compared to those of a reference polymer counterpart. For specific compounds, the percentage of remnant orientation is also higher, which makes these materials of great interest and promising alternatives to azobenzene-containing polymers for a variety of applications requiring a fast response and an absolute control over the molecular weight.

INTRODUCTION. Photochromic organic materials are of particular interest for potential applications varying from photoresponsive glasses to active materials in photonic devices such as diffraction gratings for light coupling, high speed optical switches, light waveguides and optical data storage.[1-5] Among the organic photochromic materials, azobenzene-containing materials are well known to undergo selective, reversible and stable *E-Z* isomerization upon irradiation with appropriate wavelengths.[6,7] The low fatigability of the isomerization reaction over more than 10^6 cycles has led to intense activity in the past two decades in the field through the fabrication of a variety of devices encompassing surface relief gratings with linear and nonlinear optical properties,[8-11] mechanical actuators,[12-14] sensors,[15-17] media for optical data-storage,[5,18] and other photonic devices such as waveguides,[19,20] distributed feedback lasers[21,22] and nanoplasmonic assemblies.[23] Azopolymers present the particular advantage to be easily processed in thin films and to yield a high and stable degree of orientation upon selective irradiation with polarized light.[24] However, key parameters such as the response time, the degree of photoinduced orientation and the remnant orientation can significantly be improved to reach faster dynamics, larger and more stable orientation, thus opening new applications where these parameters are critical such as optical data storage media.[5,25] Up to now, most of the orientation studies have been devoted to side-chain amorphous and liquid crystalline azopolymers where cooperative side chain effects and entanglement from the polymer backbone rule most prominently the dynamic of the molecular rearrangement upon light excitation. To enable a higher level of photoinduced orientation, a variety of optimized molecular structures of low molecular-weight copolymers have been developed by several groups to enhance the cooperative molecular motion between a photoactive unit and a non-photoactive non-absorbing unit[26,27] or between two distinct mesogenic units that serve as antenna for the incident light.[28,29] Levels of birefringence as high as

0.2 were reported in liquid-crystalline polymers enabling a vivid interest for data storage applications although the molecular orientation rates were too slow for high throughput applications. Entanglement from the polymer backbone is a critical parameter that is presumably responsible of an inhomogeneous distribution of the orientation and relaxation rates of the photoactive units thus slowing down the orientation dynamic of the azo chromophores. Such effects have been investigated at a molecular level using polarization modulation infrared spectroscopy linear dichroism (PM-IRLD) on amorphous, semi-crystalline and liquid crystalline polymers.[30-32] In these pump-probe experiments the photoinduced linear dichroism was investigated during cycles of orientation and relaxation. Since PM-IRLD provides a quantitative information on each IR active vibrational modes, it was possible to investigate dynamically the orientation of the individual vibrations. Quantification of the ordering of vibrational modes with defined symmetry could be performed and was used to determine cooperative effects between the side groups of the azopolymers chains. For modes with rather undefined symmetry, PM-IRLD was key to provide clues about their involvements in the molecular orientation process showing in particular that the backbone of the polymer conserve an isotropic conformation meanwhile it affects the rate of the molecular orientation.

In this context, molecular materials made of small organic molecules offer a very interesting alternative to polymer materials since there is no need of dilution of the photochromes within a polymer binder to avoid crystallization or aggregation of the molecules.[33] These small molecules can form pristine amorphous glasses and thin films, and, due to the absence of polymer-chain entanglement, faster photo induced dynamics are observed as reported for the fabrication of surface relief gratings.[34-37] Such materials often based on a bulky electron-donor group such as triphenylamine, diaminobiphenyl or triarylamine have been investigated in a varied of

applications such as electroluminescent devices,[38,39] organic electronic memory device[40,41] and optical glasses with nonlinear optical properties.[42]

Herein, we report on the dynamical study of a series of nine push-pull azo derivatives whose structure, based on a triarylaminoazo core, has been substituted with various electron-withdrawing groups to assess the effect of the substituent onto the molecular orientation capability in glassy thin films. The photoinduced birefringence was dynamically measured over several cycles of irradiation and thermal relaxation. To complement the macroscopic response provided by the birefringence measurements, the molecular orientation of the individual chemical groups was dynamically recorded for the nine compounds with PM-IRLD giving a clearer view on the orientation of the triphenylaminoazo molecules. All birefringence and PM-IRLD measurements were compared against thin films of poly[4'-(((2-(methacryloyloxy)ethyl)ethyl)-amino)-4-nitroazobenzene-co-Methyl methacrylate] with DR1M mole fraction of 0.11 and thus referred as pDR1M-11% or more simply pDR1M in this manuscript. This compound is considered as the archetype of push-pull azo dye and subjected to numerous fundamental and applied studies.[10,43-47] The rates of orientation and relaxation, as well as the degree of orientation were systematically determined by fitting the birefringence evolution using bi-exponential laws and compared against those obtained from pDR1M thin films. We show that the rate of orientation in some compounds can be enhanced by a 7-fold factor. The degree of orientation is however smaller than for azopolymers, yet with a higher residual orientation upon relaxation, in particular for the compounds substituted with bulkier groups like carbazolyl ones. These materials with faster response can be valued for a variety of applications where faster switching time is an essential criterion.

EXPERIMENTAL METHODS.

Preparation of thin films. The solutions were prepared using a 2 % solution of the azo compound in chloroform. The solution was filtered using Micropores filters (0.2 μm-large pores) and spin-coated onto glass slides and NaCl plates for birefringence and infrared experiments, respectively. Typical thicknesses varied between 300 to 500 nm and were systematically measured by atomic force microscopy (AFM). The properties of the thin films are reported in Table 1**.**

Birefringence. The setup is described in Figure 1A**.** The probe beam consisted in a He-Ne laser at 632.8 nm (1 mW) and its incidence was set normal to the sample. The pump beam was set at 532 nm with an irradiance of 80 mW/cm^2 and with an incidence of 15 degrees with respect to the sample normal direction. A fast photodiode was used to detect the phase shift $\Delta\varphi$ between the two main axes of the film, with a temporal resolution of about 100 ms. The phase shift was calibrated with a Babinet-Soleil compensator and the absolute birefringence was determined knowing the probe wavelength λ, and the thickness *d*, of the thin films using Equation (1):

$$\Delta n = n_{//} - n_{\perp} = \frac{2\pi d \Delta\varphi}{\lambda} \qquad (1)$$

where $n_{//}$ and $n_{\perp}$ are the refractive indices in the planes parallel and perpendicular to the pump beam polarization direction, respectively. Experiments were done in triplicates on different films.

Polarization Modulation Infrared Linear Dichroism Spectroscopy. The setup is described in Figure 1B. A mid-IR source from a Fourier-Transform spectrometer is directed outside the spectrometer and modulated between two orthogonal polarization directions noted // and ⊥ at a frequency of 74 kHz using a photoelastic modulator (Hinds). The signal detected by a MCT-A detector is electronically filtered and amplified using a lock-in amplifier and, after processing, is equal to the dichroic spectrum, namely $\Delta A = A_{//} - A_{\perp}$ where A_i refers to the i-polarized

absorbance (parallel or perpendicular). The *in-situ* irradiation of the sample was performed using a 532 nm laser source enabling the recording of photoinduced dichroic spectra during several cycles of orientation followed by relaxation. Erasure was performed by adding a quarter-waveplate on the beam path. 60 spectra were recorded for a single measurement yielding a temporal averaged resolution of 1 spectrum/min. Calibration and normalization of the resulting linear dichroism ΔA were done for each spectrum that was integrated over distinct spectral domains corresponding to the different vibrational bands.[48]

RESULTS AND DISCUSSION.

The syntheses and characterizations of the investigated series of glass-forming push-pull azo derivatives were previously reported.[49] A modular approach was used, leading to the fabrication of nine azo compounds containing various bulky groups (3,5-bis(trifluoromethyl)phenyl (**CF_3**),4-*tert*-butylphenyl (**tBu**) and 4-bis*(4-tert*-butyl)carbazolylphenyl (**Carb**) and electron-withdrawing units such as the NO_2, CN and CO_2Me groups (Scheme 1). The push-pull structure along the azo core provides a large charge transfer from the amino group in the triarylamine to the electron-accepting group, thereby yielding an electronic transition located in the visible range which is a superimposition of π-π* and n-π* transitions. For the present series, the maximum absorption wavelengths of the thin films vary between 450 nm to 500 nm as summarized in Table 1. In order to trigger the photoinduced isomerization, resonant light is generally used. In the present study, we have used a 532 nm excitation light that was linearly polarized. This excitation wavelength is resonant or pre-resonant with most of the electronic transitions of the push-pull azo compounds. Nevertheless for **CF_3CO_2Me**, weaker interactions are expected due to the large difference between absorption (445 nm) and excitation (532 nm). Beside the photoisomerization

process that has been thoroughly investigated in toluene solution,[49] a stable angular reorientation of the azo molecules occurs in thin films. This angular hole-burning is a consequence of the molecular reorientation of the azo compounds through a rotation around the N=N bond upon excitation with polarized light.[50,51] Such phenomenon is of particular interest in thin films since it yields large anisotropic properties which can be probed using polarized light. Here below, we have thus investigated the response of such thin films subjected to irradiation with a polarized light set at 532 nm.

Birefringence measurements during an orientation and a relaxation cycle. In order to probe the macroscopic response of the azo series under irradiation at 532 nm, birefringence measurements were performed at 632.8 nm for all nine triphenylaminoazo compounds as well as for the reference **pDR1M** thin film (Fig. 2A-D). The absolute values of the measured birefringence $|\Delta n|$ were shown in Figure 2. The dynamics of orientation and relaxation are reported on the same figure for a selected electron-donating group and various electron acceptors. Figures 2A, 2B and 2C report the dynamics within a series of azo derivatives containing the same bulky substituents (tBu, CF_3 and Carb, respectively) while Figure 2D features the dynamics for the reference **pDR1M** thin film. All figures are drawn with the same scales, emphasizing that both the maximum birefringence $|\Delta n|_{max}$ upon irradiation and the remnant one $|\Delta n|_{\infty}$ after relaxation are higher for a **pDR1M** thin film compared to the triphenylamino series. In order to extract the rate constants k_i associated with the dynamics of the birefringence measurements during both the orientation and relaxation processes, biexponential fitting laws were used as already reported for the photochromic studies in thin films.[35,49,52] The orientation processes are described by Eq.(2),

$$y_{orientation}(t) = m_1^{or} e^{-k_1^{or} t} + m_2^{or} e^{-k_2^{or} t} + m_3^{or} \qquad (2)$$

while the relaxation is described by Eq.(3).

$$y_{relaxation.}(t) = m_1^{rel}\left(1 - e^{-k_1^{rel} t}\right) + m_2^{rel}\left(1 - e^{-k_2^{rel} t}\right) + m_3^{rel} \qquad (3)$$

Such biexponential models are particularly well adapted to describe the dynamic orientation in azo materials where k_1^{or} and k_1^{rel} are the fast rate constants associated with the *E-Z* and Z-E isomerization processes respectively, and are convoluted with the mechanical and thermal responses of the matrix. k_2^{or} and k_2^{rel} are the slow rate constants associated with the angular redistribution of the *E* species at longer time during the orientation and the relaxation processes. In thin films, both $k_1^{or,rel}$ and $k_2^{or,rel}$ depend on the inhomogeneity effects from the matrix. In addition to the rate constants, $m_3^{or,rel}$ is a fitting variable that can be used to appreciate the level of birefringence at the plateau value during the orientation or the remnant birefringence upon relaxation while the values of $m_1^{or,rel}$ and $m_2^{or,rel}$ provide the weight of the fast and slow rate constants during the dynamics.

The fitting parameters for the orientation and relaxation processes associated to the birefringence curves shown in Figure 2A-D are reported in Tables 1 and 2, for the orientation and relaxation processes, respectively. The maximum level of photoinduced birefringence can be measured for **tBuCN** and **CarbNO₂** with $|\Delta n|$ = 0.0283 and $|\Delta n|$ = 0.0317, respectively. These values have to be compared with $|\Delta n|$ = 0.0458 for **pDR1M**. It is noteworthy that **tBuNO₂** is also among the materials yielding the largest birefringence with $|\Delta n|$ = 0.0252. Importantly, the rate constant k_1^{or}

associated with the faster contribution is significantly larger for **tBuCN** and **tBuNO$_2$** as compared to **pDR1M**, with an increase by a factor of 5.7 and 7 respectively. This indicates that the photoisomerization reaction is facilitated in the molecular thin films made of the triphenylamino azo derivatives as compared to polymer thin films where the movement of azo units is hindered by the polymer backbone. In agreement with the faster orientation reported for **tBuCN** and **tBuNO$_2$** during the orientation cycle, the remnant birefringence is also found among the smallest one for **tBuCN** and **tBuNO$_2$**. This implies that a material that shows faster photoinduced anisotropy also loses its anisotropy more readily. Nevertheless, it is difficult to observe a trend on the dominant rate constant during the relaxation process. For the polymer sample, the weights of the two rate constants are close to each other (m_1^{rel} = 46.2 % while m_2^{rel} = 53.8 %) while in the molecular thin films of the triphenylamino azo compounds the slow rate constant is at least 3 times larger than the fast rate constant. This indicates that the relaxation process is mainly driven by the angular redistribution of the *E* isomers when the irradiation light is switched off. This is different from the orientation cycle where all dynamics are mainly driven by the fast rate constant for both types of materials.

Other compounds that are poorly absorbing the 532 nm radiation such as **CF$_3$CN** also show faster orientational rate constant (k_1^{or} = 8.450 s^{-1}) even though the induction of the photoisoimerization reaction is not optimized in terms of excitation-absorption match. This trend shows clearly that when the rate photoisomerization is improved, its relaxation will also be facilitated yielding a weaker residual birefringence. This emphasizes that an ideal azo-containing material that presents a fast response time, a high degree of photoinduced birefringence and a high residual birefringence must display a subtle balance between its surrounding free volume, its associated glass transition temperature and its absorption coefficient at the excitation

wavelength. Mixtures or doped systems may be a valuable approach to improve both rates and level of photoinduced orientation. The proper selection of a material for a given application is also critical. For example, one may not need a very high level of birefringence (i.e. $|\Delta n| = 0.2$) in optical data storage application since the optical read-out can be done with high sensitivity with a much lower intrinsic birefringence but the speed (rate) of the induced birefringence is the most critical for high-density storage. The triphenylaminoazo compounds such as **tBuCN** or t**BuNO$_2$** can therefore be valued for their response time significantly faster than that for the **pDR1M** polymer. The degree of birefringence is still large and can be detected easily making molecular thin films interesting organic systems for fast optical switching.

Birefringence Stability to Cycling.

Further birefringence experiments were conducted to evaluate the behavior of the nine compounds when subjected to several cycles of irradiation. The results are reported in Figure 2E for **tBuNO$_2$** and **CarbCO$_2$Me** molecular thin films that were selected due to their faster orientation. The response over five cycles is consistent for both the orientation and relaxation processes. The compound **CarbCO$_2$Me** shows a birefringence of Δn= -0.0192 and a residual birefringence of Δn = -0.0168 after 250 s of relaxation, which yields 81 % of remnant birefringence that is higher than that of any other compounds of this study. Remarkably, all **Carb** compounds have a high degree of residual anisotropy ranging from 68 % (**CarbNO$_2$**), which is comparable to that for **pDR1M** (68.9 %), to 81% (**CarbCO$_2$Me**) as summarized in Table 2. This emphasizes again that even though a smaller degree of order is induced, our materials have a faster response time compared to pDR1M and yet can have the same level of percentage of residual birefringence. The ability of these compounds to yield reversible and

erasable photoinduced anisotropy was investigated using circularly polarized light. After a cycle of orientation-relaxation, the residual anisotropy was erased using a circularly polarized 532 nm beam for 100 s. The results are shown in Figure 2F for two consecutive cycles for **tBuNO$_2$,** **CarbNO$_2$** and **CarbCO$_2$Me**. For all compounds, the anisotropy was erased completely to zero and after a second irradiation the induction of anisotropy is comparable to the initial cycle. One can however notice a slight continuous increase in the plateau of birefringence for **CarbCO$_2$Me** after each irradiation cycle, which lets us suggest progressive plasticization of the thin films. Rotation of the **Carb** azo units operates in one block and requires enough space due to the bulky **Carb** units, which can thus be achieved only after repetitive cycles of orientation-relaxation**.**

Polarization-modulation linear dichroism infrared spectroscopy. In order to investigate the photoinduced orientation at the molecular level during a cycle of orientation-relaxation, we have investigated the linear dichroism of irradiated thin films in the mid-infrared range using PM-IRLD spectroscopy. This powerful method with monolayer sensitivity has already been used successfully for the study of azobenzene-containing materials such as liquid crystalline materials as well as doped and functionalized polymer thin films.[30,32] It allows the motions of photoactive and non-photoactive units to be dynamically disentangled, thereby yielding a better appreciation of both the polarity and the steric effects associated with molecular motions.[43] The determination of the linear dichroism value $\Delta A = A_{//} - A_{\perp}$ is therefore a critical parameter to assess the orientational behavior of the azo compounds by following the evolution of their individual vibrational normal modes. This sheds light on the part of the molecule that undergoes molecular reorientation upon irradiation with a linearly polarized light. $A_{//}$ and $A_{\perp}$ refer to the polarized absorbances parallel and perpendicular to the direction of the polarized pump laser, respectively. Therefore, upon irradiation, a vibrational mode with an initial dominant component along the //

direction will experience an angular reorientation along the $\perp$ direction, yielding a negative value for ΔA. Conversely, a mode with a dominant component initially oriented along $\perp$ direction will have a positive ΔA. To obtain a quantitative information about the time-dependent behavior of the different vibrational bands associated with the triphenylaminoazo derivatives, a distribution function, F_θ, is usually defined. F_θ is proportional to the normalized dichroism ratio $\Delta A / 3A_0$ where A_0 designates the absorbance prior to irradiation for a given vibrational mode such as defined in Eq. [4]. In azo materials the distribution function is model-dependent so that both uniaxial and biaxial models can be used to accurately quantify the level of photoinduced orientation.[31] In uniaxial orientation models, the molecular orientation can be described using a single angle θ that describes the orientation of the long molecular axis of the chromophore with respect to the polarized excitation. This model implies that rod-like molecules can orient perpendicularly to the excitation light within the plane of the film or out-of-the-plane direction (i.e. along the beam propagation direction) with the same probability. In bi-axial models, the orientation is more complex to describe since the rod-like molecules do not have the same probability to orient along the plane and out-of-plane directions. Therefore, two angles θ and ϕ must be used to define the orientational parameters associated with such anisotropic molecular orientation.[53] Based on previous studies performed in azo polymers containing a low concentration of dyes, an uniaxial model is generally appropriate, while for higher dye concentrations, biaxial models provide more accurate description of the molecular orientation. In the present study, separated measurements of polarized $A_{//}$ and $A_\perp$ were initially performed (Supplementary information SI1) confirming that the chromophore orientation can be accurately described by an uniaxial model for the study of vibrational modes with well-defined symmetry such as symmetric stretching mode of NO_2 (SI1). Although the high density of azo molecules

would be in favor of a biaxial-type orientation, the large size of the chromophores together with a larger free volume around each individual chromophore are presumably the critical parameters that yield an uniaxial orientation. Therefore, in the present study the uniaxial model is valid for the present molecular materials and the distribution function can be described by:

$$F_\theta = \frac{A_{//} - A_\perp}{3A_0} = \frac{\Delta A}{3A_0} \qquad (4)$$

Using the uniaxial distribution, the F_θ parameter is equivalent to the second order Legendre polynomial also defined as the second order parameter $\langle P_2 \rangle = \frac{1}{2}\langle 3\cos^2\theta - 1 \rangle$. In the case of a uniaxial distribution function, the limit values are F_θ = 1 for a perfect alignment along the // direction ($\theta = 0$) and F_θ = -0.5 for a perfect alignment in the $\perp$ direction ($\theta = \frac{\pi}{2}$) while F_θ = 0 indicates an isotropic material.

Here below, we have measured the photoinduced anisotropy for the nine azo triphenylamino compounds and the azo reference polymer. Selected dynamics for **tBuNO$_2$** and **CarbNO$_2$** are shown in Figures 3 and 4 while the measurements for all other compounds and **pDR1M** thin films are shown in the supplementary information section (SI2-9) for selected vibrational modes. The vibrational assignments are summarized in the supplementary information section (SI 10). Because of the high amount of aromatic cycles and the overall geometry of the molecules, the vibrational modes associated with the aromatic cycles such as the deformation modes C-H of the phenyl rings, δ (1107 and 1136 cm^{-1}), and the elongation modes of the C=C, ν_{8a} (1600 cm^{-1}) and ν_{8b} (1588 cm^{-1}), do not present a well-defined symmetry and are therefore not ideal probe groups to estimate a clear-cut molecular orientation. Nevertheless this observation is also true for

azopolymers studies where limited number of groups on the donor side or the polymer backbone had a well defined symmetry and could be exploited to provide information about the electron donor group orientation. Generally the degree of orientation of the $\nu_{8a} + \nu_{8b}$ phenyl elongation modes are very close in magnitude to the symmetric stretching mode of the nitro group as shown in the supplementary information section for pDR1M (SI9). Such observation can be used as a reference to evaluate the influence of the bulky donor group. Other modes display better defined symmetry in particular on the electron-accepting side of the chromophore. For example, the symmetric ν_S (1343 cm^{-1}) and antisymmetric ν_{as} (1516 cm^{-1}) modes of the nitro group are perpendicular to each other and should therefore show different signs in anisotropic systems. The symmetric mode of NO_2 is oriented along the long axis of the chromophore and can be efficiently used to follow the orientational dynamics of the chromophore. Also, modes such as νPh-N (1294 cm^{-1}) or coupled modes νN-N + Ph-N (1395 cm^{-1}) also present a larger net dipolar moment along the main molecular axis. For the series containing a cyano group, the stretching mode νC≡N (2227 cm^{-1}) is also of interest. Although the trifluoromethyl groups $–CF_3$ show a clear spectral signature with an elongation normal mode ν_{as}(C-F) at 1054 cm^{-1}, these groups cannot be used to probe the electron donor side of the chromophores due to their relative orientation devoid of unidirectionality. As shown for **CF3CN** (SI6) and **CF3NO2** (SI8), the symmetric and antisymmetric $-CF_3$ modes are clearly observable on the IR spectra but only very weak net molecular orientation of these two modes can be measured. The four CF3 groups located on the donor side have a large range of angular net contributions and the average of their orientation appears to yield very little dichroism. Alternatively, if CF_3 was substituted in R^1 position rather than R^2 (Scheme 1) larger dichroism could presumably be observed since the angular distribution would be narrower.

The linear dichroic spectra (ΔA) in the [1000-1700] cm^{-1} spectral range prior to irradiation, at the orientation plateau upon light exposure and after a long relaxation time are presented in Figures 4 and 5 for **tBuNO$_2$** and **CarbNO$_2$**, respectively (Figures 3A and 4A), along with the corresponding time-evolution of the amplitude of selected modes (Figures 3B and 4B). The ΔA spectra are superimposed with the reference absorption spectrum recorded on the same sample area prior to irradiation. In the case of **tBuNO$_2$** thin films (Figure 3A), most vibrational modes are negative indicative of an angular orientation of the vibrational mode perpendicular to the irradiation polarization direction. This also highlights that most vibrational modes have a strong contribution of their dipole moment along the long axis of the molecule such as $\nu_s NO_2$. Concomitantly, vibrational modes that have a neat vibrational symmetry oriented perpendicularly to the long molecular axis have a positive linear dichroism such as $\nu_{as} NO_2$ which is the only mode exhibiting a positive anisotropy as seen in Figures 3A and 4A. From Figures 4B and 4B, the orientational dynamics can be investigated. We thus can clearly see that the plateau of orientation is reached within the first 1-3 minutes of irradiation for both compounds. The level of induced linear dichroism yields values of $F_\theta = -0.045$ and $F_\theta = -0.07$ for **tBuNO$_2$** and **CarbNO$_2$**, respectively, while for the **pDR1M** thin film, the value is larger with $F_\theta = -0.13$. It is noteworthy that for **CarbNO$_2$,** the C=C vibrations experience the most anisotropy. This indicates clearly that the electron-accepting group and the electron-donating group that holds the carbazole units undergo simultaneous angular reorientations. The donor unit being very bulky, this confirms that a larger free volume occupied by the donor unit has been created during the angular reorientation of the azo unit facilitating the orientation of the surrounding units and thus explaining the faster orientation and relaxation rates. This also confirm that the position of the carbazole groups on R^1 (Scheme 1) yields a larger dichroism as pointed out earlier than for the -

CF_3 groups positioned on R^2. This observation corroborates the fact that the chromophore orients as a whole unit in the perpendicular direction to the impinging polarization direction. The remnant linear dichroism confirms the birefringence measurements previously recorded and shows that for fast-responsive azo chromophores, the induced dichroism is lower while the decay of dichroism is faster due to the increased amount of free volume induced by the bulky donor substituent. Interestingly, in the case of the **CarbNO2**, the relaxation never reaches a steady state even after one hour of relaxation as shown in Fig.5A for the NO_2 group. This indicates that there is a large distribution of free volume that are involved during the relaxation which is presumably due to the position of the carbazole groups with respect to the phenyl group to which they are attached in R^1. Rotation of the Carbazole group presumably lead to a larger distribution of free volume sizes on the donor side of the chromophore. Upon thermal back-relaxation process, the orientation of the chromophore is affected by such distribution of free volume and broader inhomogeneous effect from the glassy material, explaining reduced rate of relaxation.

In Figure 5A, we have reported the linear dichroism dynamics of the NO_2 band for the three triphenylaminoazo compounds together with **pDR1M**. Several factors such as the glass transition temperatures T_g and the absorption cross sections of the material must be carefully examined for comparison. For the four compounds, the maximum absorption wavelengths are about 490 ± 20 nm and their molar absorption coefficients in solution exhibit very similar values of 27.0×10^3, 30.5×10^3 and 24.6×10^3 $mol^{-1}.L.cm^{-1}$ for **$tBuNO_2$, $CarbNO_2$** and **CF_3NO_2**, respectively and 30×10^3 for **pDR1M** thin film. The glass transition temperatures T_g are however very distinct for the three triphenylaminoazo compounds ranging from 62 ºC for **CF_3NO_2** to 202 ºC for **$CarbNO_2$** while **$tBuNO_2$** and **pDR1M** have a T_g around 110 ºC. The comparative experiments carried out on this series show no direct correlation between T_g: indeed **pDR1M** shows the highest degree of

orientation while **tBuNO$_2$** shows the smallest orientation that is comparable to the **CF$_3$NO$_2$** one. Conversely, **CarbNO$_2$** shows an intermediate level of anisotropy as observed in birefringence measurements even though it has a higher glass transition temperature. This shows again the importance of microscopic free volume accessible in the triphenylaminoazo derivatives highlighting the fact that angular reorientation can be very effective even for high T_g materials endowed with bulky substituents as already demonstrated for the formation of surface relief gratings.[8,49] Figure 5B shows the series of azo molecules substituted with a CN group as an electron acceptor. Here again the same trend is observed: the **CarbCN** compound (T_g = 201 ºC) shows a highest level of anisotropy compared to those of **tBuCN** (T_g = 117 ºC; Supplementary information SI2) and **CF$_3$NO$_2$** (T_g = 68 ºC; Supplementary information SI8). Figure 5C shows the anisotropy associated with the C=O stretching mode (ν_s C=O, 1731 cm^{-1}) of the azo ester molecules containing the methoxycarbonyl group –CO$_2$Me as an electron-withdrawing substituent. A poor level of anisotropy and noisy signals are due to the weak band intensity but the trend is again the same, namely bulkier substituents yield larger anisotropy.

CONCLUSION

In conclusion, we have probed the dynamics associated with the angular reorientation of triphenylaminoazo dyes using birefringence and polarization modulation infrared spectroscopy. These complementary approaches provided valuable set of macroscopic and molecular information during the angular photoinduced molecular reorientation. The fast rate constants associated with the photoinduced anisotropy are enhanced for the whole series of compounds compared to a reference azopolymer. This indicates that the dynamics within molecular glassy thin films can be significantly improved by tuning the size of the electron donor group with substituents of varying bulkiness. Several candidates of the series show improved properties like

the carbazole series that exhibit a higher level of photoinduced and remnant anisotropy whereas their glass transition temperature is above 200 ºC. The **tBu** series shows an enhanced orientation rate by a factor of 7 despite similar glass transition temperatures to the reference azopolymer. This study shows clear evidence that small molecule-based thin films of azo compounds exhibit dynamical properties exceeding those of polymers doped or functionalized with azobenzene groups. This study demonstrate that molecular functional materials display larger orientational rates with regard to those of their polymer analogues, which can impact considerably the choice for polymer- or small molecule-based technologies encountered in the field of organic electronics and photonics.

ASSOCIATED CONTENT

Supporting Information. Polarization modulation spectra and dynamics of all compounds. This material is available free of charge via the Internet at http://pubs.acs.org.

AUTHOR INFORMATION

Corresponding Author

*flagugne@uwo.ca

Author Contributions

The manuscript was written through contributions of all authors. All authors have given approval to the final version of the manuscript.

Notes

The authors declare no competing financial interest.

ACKNOWLEDGMENTS

The France-Canada Research Fund and the French Ministry of Foreign Affairs are gratefully acknowledged for their financial support and the funding of a France-Canada co-tutelle PhD grant (K.E.S). The French National Agency of Research is also strongly acknowledged for his financial support through the ANR 2010 BLANC 1004 03_COME-ON project. F.L.-L. acknowledges the NSERC Discovery Grant and Research Tool and Instrumentation programs.

REFERENCES

(1) Priimagi, A.; Lindfors, K.; Rochon, P. Efficient Surface-Relief Gratings in Hydrogen-Bonded Polymer−Azobenzene Complexes. *ACS Appl. Mater. Interfaces* **2009**, *1*, 1183-1189.

(2) Delaire, J. A.; Nakatani, K. Linear and nonlinear optical properties of photochromic molecules and materials. *Chem. Rev.* **2000**, *100*, 1817-1846.

(3) Gust, D.; Andréasson, J.; Pischel, U.; Moore, T. A.; Moore, A. L. Data and signal processing using photochromic molecules. *Chem. Commun.* **2012**, *48*, 1947-1957.

(4) Matharu, A. S.; Jeeva, S.; Ramanujam, P. S. Liquid crystals for holographic optical data storage. *Chem. Soc. Rev.* **2007**, *36*, 1868-1880.

(5) Hagen, R.; Bieringer, T. Photoaddressable Polymers for Optical Data Storage. *Adv. Mater.* **2001**, *13*, 1805-1810.

(6) Neporent, B. S.; Stolbova, O. V. Reversible orientational photodichroism in viscous solutions of complex organic substances. *Opt. Spektrosk.* **1963**, *14*, 624-633.

(7) Makushenko, A. M.; Neporent, B. S.; Stolbova, O. V. Reversible Photodichroism and photoisomerization of complex organic compounds in viscous solutions. II. Azobenzene ands substituted derivatives of azobenzene. *Opt. Spektrosk.* **1971**, *31*, 741-748.

(8) Ishow, E.; Camacho-Aguilera, R.; Guerin, J.; Brosseau, A.; Nakatani, K. Spontaneous Formation of Complex Periodic Superstructures under High Interferential Illumination of Small-Molecule-Based Photochromic Materials. *Adv. Funct. Mater.* **2009**, *19*, 796-804.

(9) Di Florio, G.; Brundermann, E.; Yadavalli, N. S.; Santer, S.; Havenith, M. Graphene Multilayer as Nanosized Optical Strain Gauge for Polymer Surface Relief Gratings. *Nano Lett.* **2014**, *14*, 5754-5760.

(10) Lagugné-Labarthet, F.; Buffeteau, T.; Sourisseau, C. Optical erasures and unsusual surface reliefs of holographic gratings inscribed on thin films of an azobenzene funxtionalized polymer. *Phys. Chem. Chem. Phys.* **2002**, *4*, 4020-4029.

(11) R. D. Schaller, R. J. S., Y. R. Shen, F. Lagugné-Labarthet Poled polymer thin-film gratings studied with far-field optical diffraction and second-harmonic near-field microscopy. *Opt. Lett.* **2003**, *28*, 1296-1298.

(12) Yu, Y.; Nakano, M.; Ikeda, T. Photomechanics: Directed bending of a polymer film by light. *Nature* **2003**, *425*, 145.

(13) Yamada, M.; Kondo, M.; Mamiya, J.; Yu, Y.; Kinoshita, M.; Barrett, C. J.; Ikeda, T. Photomobile Polymer Materials: Towards Light-Driven Plastic Motors. *Angew. Chem. Int. Edit.* **2008**, *47*, 4986-4988.

(14) Liu, Z.-X.; Feng, Y.; Yan, Z. C.; He, Y.-M.; Liu, C.-Y.; Fan, Q.-H. Multistimuli Responsive Dendritic Organogels Based on Azobenzene-Containing Poly(aryl ether) Dendron. *Chem. Mater.* **2012**, *24*, 3751-3757.

(15) Mermut, O.; Barrett, C. J. Stable sensor layers self-assembled onto surfaces using azobenzene-containing polyelectrolytes. *Analyst* **2001**, *126*, 1861-1865.

(16) Zakrevskyy, Y.; Stumpe, J.; Faul, C. F. A Supramolecular Approach to Optically Anisotropic Materials: Photosensitive Ionic Self-Assembly Complexes. *Adv. Mater.* **2006**, *18*, 2133-2136.

(17) Joshi, G. K.; Blodgett, K. N.; Muhoberac, B. B.; Johnson, M. A.; Smith, K. A.; Sardar, R. Ultrasensitive Photoreversible Molecular Sensors of Azobenzene-Functionalized Plasmonic Nanoantennas. *Nano Lett.* **2014**, *14*, 532-540.

(18) Holme, N. C. R.; Ramanujam, P. S.; Hvilsted, S. 10,000 optical write, read, and erase cycles in an azobenzene sidechain liquid-crystalline polyester. *Opt. Lett.* **1996**, *21*, 902-904.

(19) Stockermans, R. J.; Rochon, P. L. Narrow-band resonant grating waveguide filters constructed with azobenzene polymers. *Appl. Opt.* **1999**, *38*, 3714-3719.

(20) Priimagi, A.; Shevchenko, A. Azopolymer-Based Micro- and Nanopatterning for Photonic Applications. *J. Polym. Sci., Part B: Polym. Phys.* **2014**, *3*, 163-182.

(21) Goldenberg, L. M.; Lisinetskii, V.; Gritsai, Y.; Stumpe, J.; Schrader, S. Single Step Optical Fabrication of a DFB Laser Device in Fluorescent Azobenzene-Containing Materials. *Adv. Mater.* **2012**, *24*, 3339-3343.

(22) Goldenberg, L. M.; Lisinetskii, V.; Ryabchun, A.; Bobrovsky, A.; A., S. Liquid Crystalline Azobenzene-Containing Polymer as a Matrix for Distributed Feedback Lasers. *ACS Photonics* **2014**, *1*, 885-893.

(23) Snell, K. E.; Mevellec, J.-Y.; Humbert, B.; Lagugné-Labarthet, F.; Ishow, E. Photochromic Organic Nanoparticles as Innovative Platforms for Plasmonic Nanoassemblies. *ACS Appl. Mater. Interfaces* **2015**, *7*, 1932-1942.

(24) Shimamura, A.; Priimagi, A.; Mamiya, J.-I.; Ikeda, T.; Yu, Y.; Barrett, C. J.; A., S. Simultaneous Analysis of Optical and Mechanical Properties of Cross-Linked Azobenzene-Containing Liquid-Crystalline Polymer Films. *ACS Appl. Mater. Interfaces* **2011**, *3*, 4190-4196.

(25) Zhao, Y.; Ikeda, T. *Smart light-responsive materials: Azobenzene-Containing Polymers and Liquid Crystals*; John Wiley & Sons: Hoboken, NJ, USA, 2009.

(26) Natansohn, A.; Rochon, P.; Pézolet, M.; Audet, P.; Brown, D.; To, S. Azo Polymers for reversible optical storage. 4. Cooperative motion of rigid groups in semicrystalline polymers. *Macromolecules* **1994**, *27*, 2580-2586.

(27) Yoneyama, S.; Yamamoto, T.; Tsutsumi, O.; Kanazawa, A.; Shiono, T.; Ikeda, T. High-performance material for holographic gratings by means of a photoresponsive polymer liquid crystal containing a tolane moiety with high birefringence. *Macromolecules* **2002**, *35*, 8751-8758.

(28) Zilker, S. J.; Huber, M. R.; Bieringer, T.; Haarer, D. Holographic recording in amorphous side-chain polymers: a comparison of two different design philosophies. *Appl. Phys. B.* **1999**, *68*, 893-897.

(29) Zilker, S. J.; Bieringer, T.; Haarer, D.; Stein, R. S.; van Egmond, J. W.; Kostromine, S. Holographic data storage in amorphous polymers. *Adv. Mater.* **1998**, *10*, 855-859.

(30) Buffeteau, T.; Natansohn, A.; Rochon, P.; Pézolet, M. Study of Cooperative Side Group Motions in Amorphous Polymers by Time Dependent Infrared Spectroscopy. *Macromolecules* **1996**, *29*, 8783-8790.

(31) Buffeteau, T.; Pézolet, M. Photoinduced orientation in azopolymers studied by infrared spectroscopy: cooperative and biaxial orientation in semicrystalline polymers. *Macromolecules* **1998**, *31*, 2631-2635.

(32) Lagugné-Labarthet, F.; Freiberg, S.; Pellerin, C.; Pézolet, M.; Natansohn, A.; Rochon, P. Spectroscopic and Optical Characterization of a Series of Azobenzene-Containing Side-Chain Liquid Crystalline Polymers. *Macromolecules* **2000**, *33*, 6815-6823.

(33) Tanino, T.; Yoshikawa, S.; Ujike, T.; Nagahama, D.; Moriwaki, K.; Takahashi, T.; Kotani, Y.; Nakano, H.; Shirota, Y. Creation of azaobenzene-based photochromic amorphous molecualr materials- synthesis, glass forming properties, and photochromic response. *J. Mater. Chem.* **2007**, *17*, 4953-4963.

(34) Kim, M.-J.; Seo, E.-M.; Vak, D.; Kim, D.-Y. Photodynamic Properties of Azobenzene molecular films with triphenylamines. *Chem. Mater.* **2003**, *15*, 4021-4027.

(35) Nakano, H.; Takahashi, T.; Kadota, T.; Shirota, Y. Formation of a Surface Relief Grating Using a Novel Azobenzene-Based Photochromic Amorphous Molecular Material. *Adv. Mater.* **2002**, *14*, 1157-1160.

(36) Nakano, H.; Tanino, T.; Takahashi, T.; Ando, H.; Shirota, Y. Relationship between molecular structure and photoinduced surface relief grating formation using azaobenzene-based photochromic amorphous molecular materials. *J. Mater. Chem.* **2008**, *18*, 242-246.

(37) Fuhrmann, T.; Tsutsui, T. Synthesis and properties of a hole-conducting photopatternable molecular glass. *Chem. Mater.* **1999**, *11*, 2226-2232.

(38) Feng, S.; Duan, L.; Hou, L.; Qiao, J.; Zhang, D.; Dong, G.; Wang, L.; Qiu, Y. A Comparison Study of the Organic Small Molecular Thin Films Prepared by Solution Process and Vacuum Deposition: Roughness, Hydrophilicity, Absorption, Photoluminescence, Density, Mobility, and Electroluminescence. *J. Phys. Chem. C* **2011**, *115*, 14278-14234.

(39) Duan, L.; Hou, L.; Lee, T.-W.; Qiao, J.; Zhang, D.; Dong, G.; Wanga, L.; Qiu, Y. Solution processable small molecules for organic light-emitting diodes. *J. Mater. Chem.* **2010**, *20*, 6392-6407.

(40) Zhuang, H.; Zhang, Q.; Zhu, Y.; Xu, X.; Liu, H.; Li, N.; Xu, Q.; Li, H.; Lu, J.; Wang, L. Effect of terminal electron acceptor strength on film morphology and ternary memory performance of triphenylamine donor based devices. *J. Mater. Chem. C* **2013**, *1*, 3816-3824.

(41) Miao, S.; Zhu, Y.; Zhuang, H.; Xiaping, X., Li, Hua, Sun, R.; Li, N.; Ji, S.; Lu, J. Adjustment of charge trap number and depth in molecular backbone to achieve tunable multilevel data storage performance. *J. Mater. Chem. C* **2013**, *1*, 2320-2327.

(42) Ishow, E.; Bellaïche, C.; Bouteiller, L.; Nakatani, K.; Delaire, J. A. Versatile synthesis of small NLO-Active Molecules Forming Amourphous materilas with spontaneous second-order NLO response. *J. Am. Chem. Soc.* **2003**, *125*, 15744-15745.

(43) Natansohn, A.; Rochon, P.; Meng, X.; Barrett, C. J.; Buffeteau, T.; Bonenfant, S.; Pézolet, M. Molecular adressing? Selective photoinduced cooperative motion of polar ester groups in copolymers containing azobenzene groups. *Macromolecules* **1998**, *31*, 1155-1161.

(44) Ho, M.-S.; Natansohn, A.; Barrett, C. J.; Rochon, P. Azo polymers for reversible optical storage. 8. The effect of polarity of the azobenzene groups. *Can. J. Chem.* **1995**, *73*, 1773-1778.

(45) Karageorgiev, P.; Neher, D.; Schultz, B.; Stiller, B.; Pietsch, U.; Giersig, U.; Brehmer, L. From anisotropic photo-fluidity towards nanomanipulation in the optical near-field. *Nat. Mater.* **2005**, *4*, 699-703.

(46) Natansohn, A.; Rochon, P.; Gosselin, J.; Xie, S. Azo polymers for reversible optical storage.1. Poly[4'-[[2-(acryloyloxy)ethyl]ethylaminol-4-nitroazobenzene]. *Macromolecules* **1992**, *25*, 2268-2273.

(47) Rodriguez, V.; Adamietz, F.; Sanguinet, L.; Buffeteau, T.; Sourisseau, C. Quantitative Determination of the Polar Order Induced under High Electric Field in Amorphous PDR1M Azobenzene Polymer Films. *J. Phys. Chem. B.* **2003**, *107*, 9736-9743.

(48) Buffeteau, T.; Lagugné-Labarthet, F.; Pézolet, M.; Sourisseau, C. Dynamics of photoinduced orientation of nonpolar azobenzene groups in polymer films. Characterization of the Cis isomers by visible and FTIR spectroscopies. *Macromolecules* **2001**, *34*, 7514-7521.

(49) Snell, K. E.; Stéphan, N.; Pansu, R. B.; Audibert, J.-F.; Lagugné-Labarthet, F.; Ishow, E. Nanoparticle Organization Through Photoinduced Bulk Mass Transfer. *Langmuir* **2014**, *30*, 2926-2935.

(50) Lagugné-Labarthet, F.; Sourisseau, C. Transient absorption spectroscopy and angular reorientation of azobenzene molecules in a DR1-doped PMMA polymer matrix. *New J. Chem.* **1997**, *21*, 879-887.

(51) Fischer, M.; El Osman, A.; Blanche, P.-A.; Dumont, M. Photoinduced Dichroism as a Tool for Understanding Orientational Mobility of Photoisomerizable Dyes in Amorphous Matrices. *Synth. Met.* **2000**, *115*, 139-144.

(52) Ishow, E.; Lebon, B.; He, Y.; Wang, X.; Bouteiller, L.; Galmiche, L.; Nakatani, K. Structural and Photoisomerization Cross Studies of Polar Photochromic Monomeric Glasses Forming Surface Relief Gratings. *Chem. Mater.* **2006**, *18*, 1261-1267.

(53) Buffeteau, T.; Lagugné-Labarthet, F.; Sourisseau, C.; Kostromine, S.; Bieringer, T. Biaxial Orientation Induced in a Photoaddressable Azopolymer Thin Film As Evidenced by Polarized UV−Visible, Infrared, and Raman Spectra. *Macromolecules* **2004**, *37*, 2880-2889.

List of Schemes and Figures

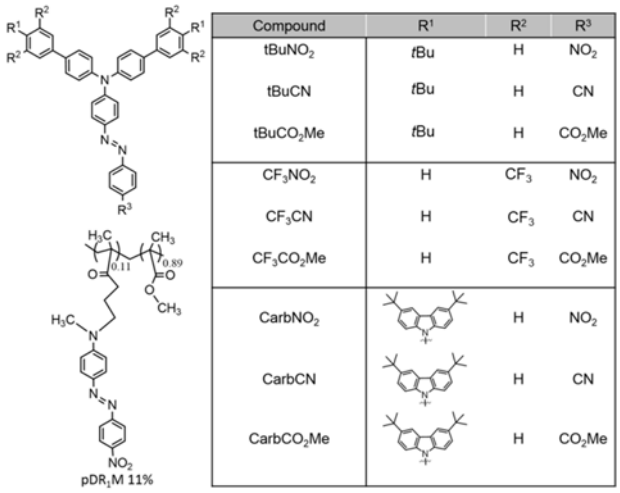

Compound	R^1	R^2	R^3
$tBuNO_2$	*t*Bu	H	NO_2
tBuCN	*t*Bu	H	CN
$tBuCO_2Me$	*t*Bu	H	CO_2Me
CF_3NO_2	H	CF_3	NO_2
CF_3CN	H	CF_3	CN
CF_3CO_2Me	H	CF_3	CO_2Me
$CarbNO_2$		H	NO_2
CarbCN		H	CN
$CarbCO_2Me$		H	CO_2Me

Scheme 1. Series of push-pull triphenylaminoazo derivatives and azo polymer **pDR1M** 11 %.

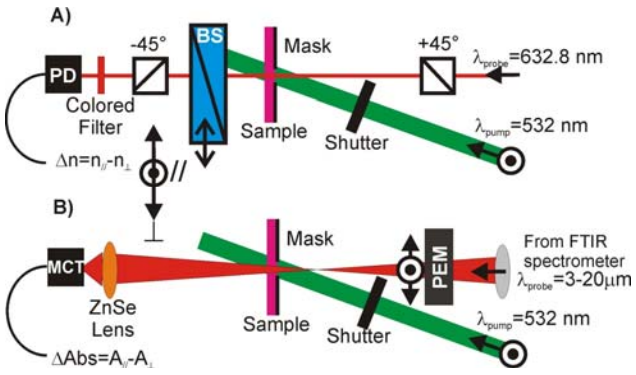

Figure 1. (A) Birefringence setup and (B) polarization modulation infrared linear dichroism setup for the study of photoinduced anisotropy in thin films.

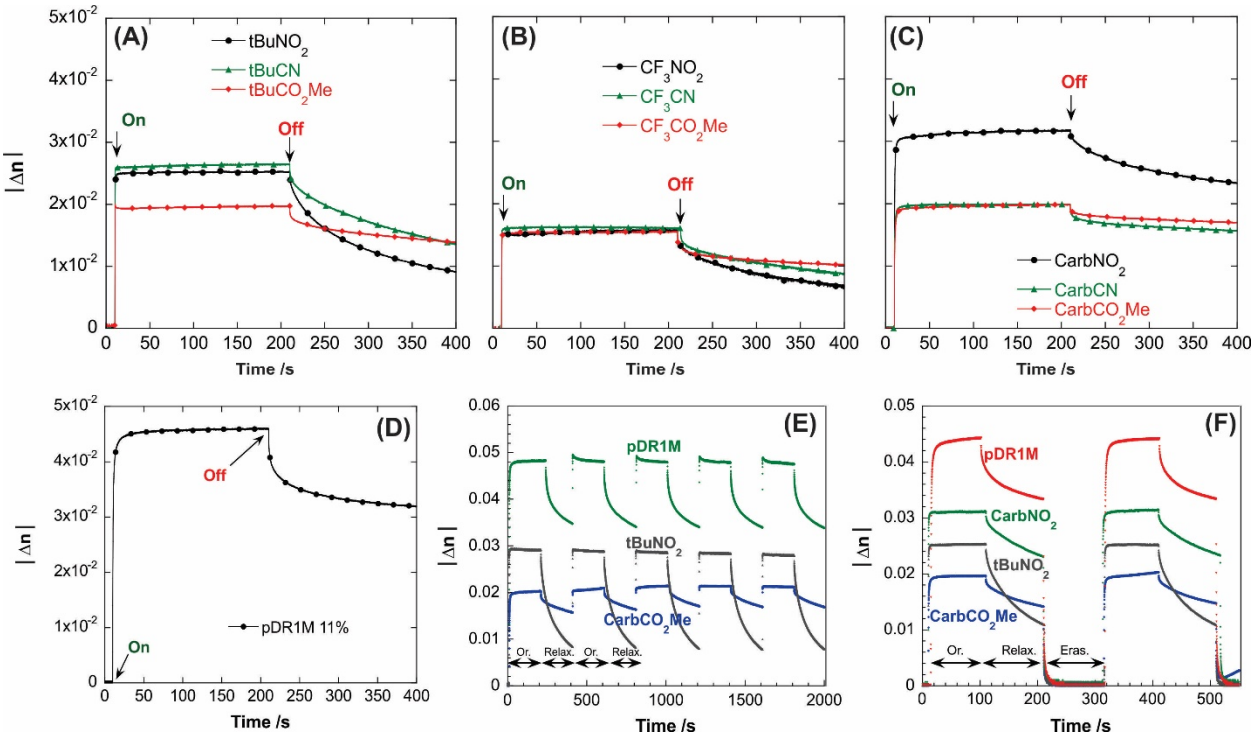

Figure 2. Birefringence dynamics during a cycle of orientation (pump on), relaxation (pump off) and erasure for the **tBu** series (A), **CF_3** series (B), **Carb** series (C) and **pDR1M** (D) processed as thin films. Cycles of orientation/relaxation for selected azo thin films of **$tBuNO_2$**, **$CarbCO_2Me$** and **pDR1M** polymer (E). Cycles of orientation, relaxation, erasure for selected azo thin films of **$CarbNO_2$**, **$tBuNO_2$**, **$CarbCO_2Me$** and **pDR1M** (F).

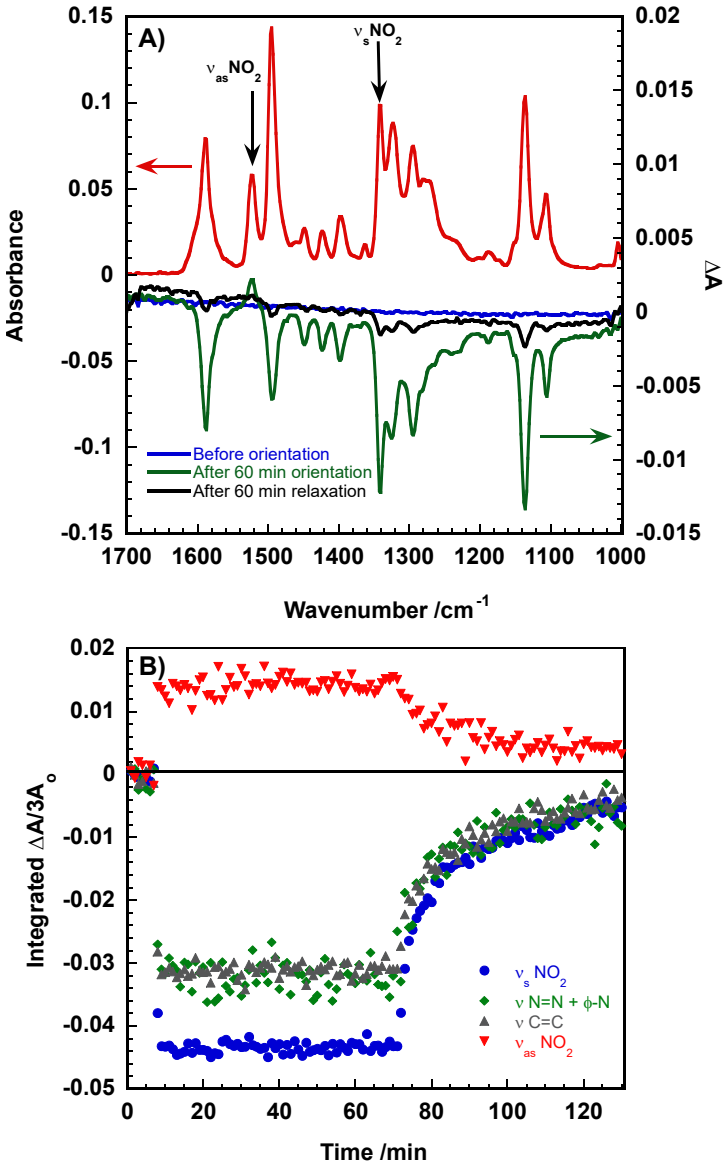

Figure 3. (A) Infrared spectrum of **tBuNO$_2$** molecular thin films and photoinduced linear dichroism at t = 0 min., after 60 min. of orientation and after 60 min. of relaxation. (B) Dynamics of selected vibrational modes such as symmetric (ν_s, 1343 cm^{-1}) and antisymmetric (ν_{as}, 1516 cm^{-1}) stretching modes of NO_2, stretching phenyl modes ν_{8a}, ν_{8b} (1600 cm^{-1} and 1588 cm^{-1}) and coupled $\nu_{N=N}+\nu_{Ph-N}$ mode (1395 cm^{-1}) during irradiation and relaxation cycles.

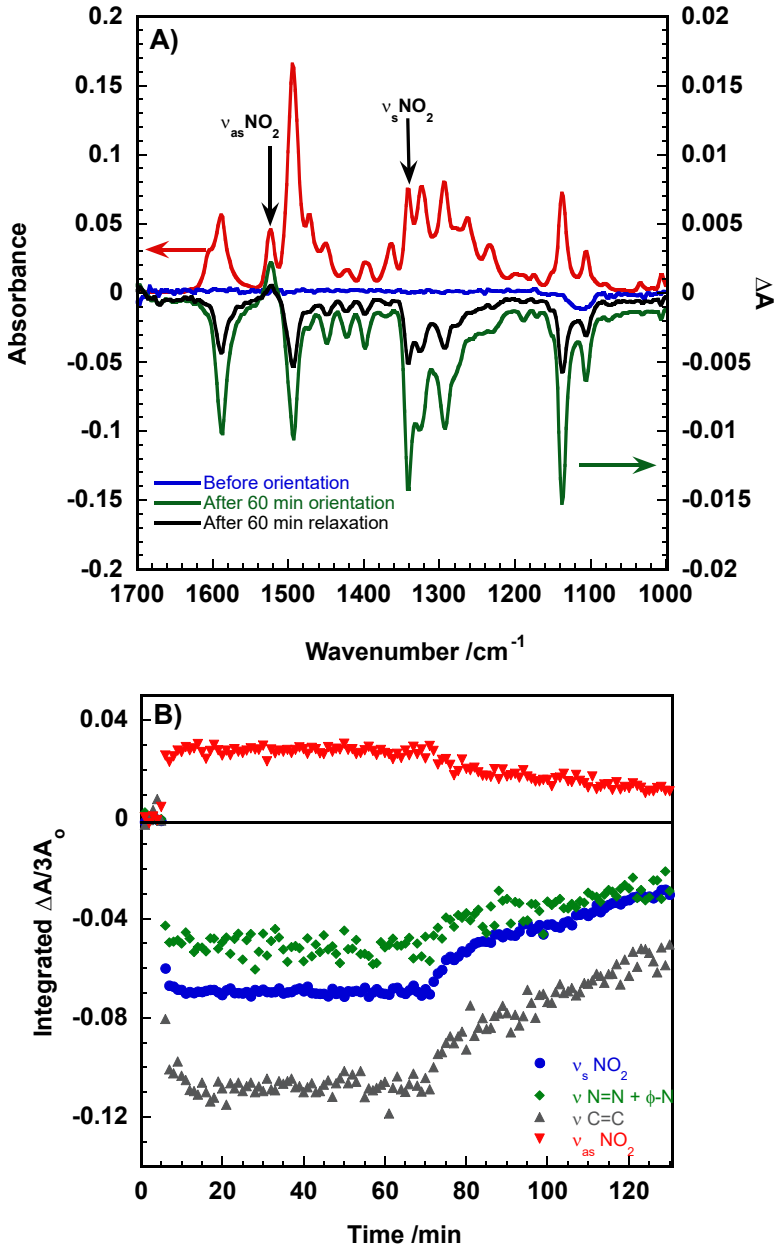

Figure 4. (A) Infrared spectrum of **CarbNO$_2$** molecular thin films and photoinduced linear dichroism at t = 0 min., after 60 min. of orientation and after 60 min. of relaxation. (B) Dynamics of selected vibrational modes such as symmetric (ν_s, 1343 cm^{-1}) and antisymmetric (ν_{as}, 1516 cm^{-1}) stretching modes of NO_2, stretching phenyl modes ν_{8a}, ν_{8b} (1600 cm^{-1} and 1588 cm^{-1}) and coupled $\nu_{N=N}+\nu_{Ph-N}$ mode (1395 cm^{-1}) during irradiation and relaxation cycles.

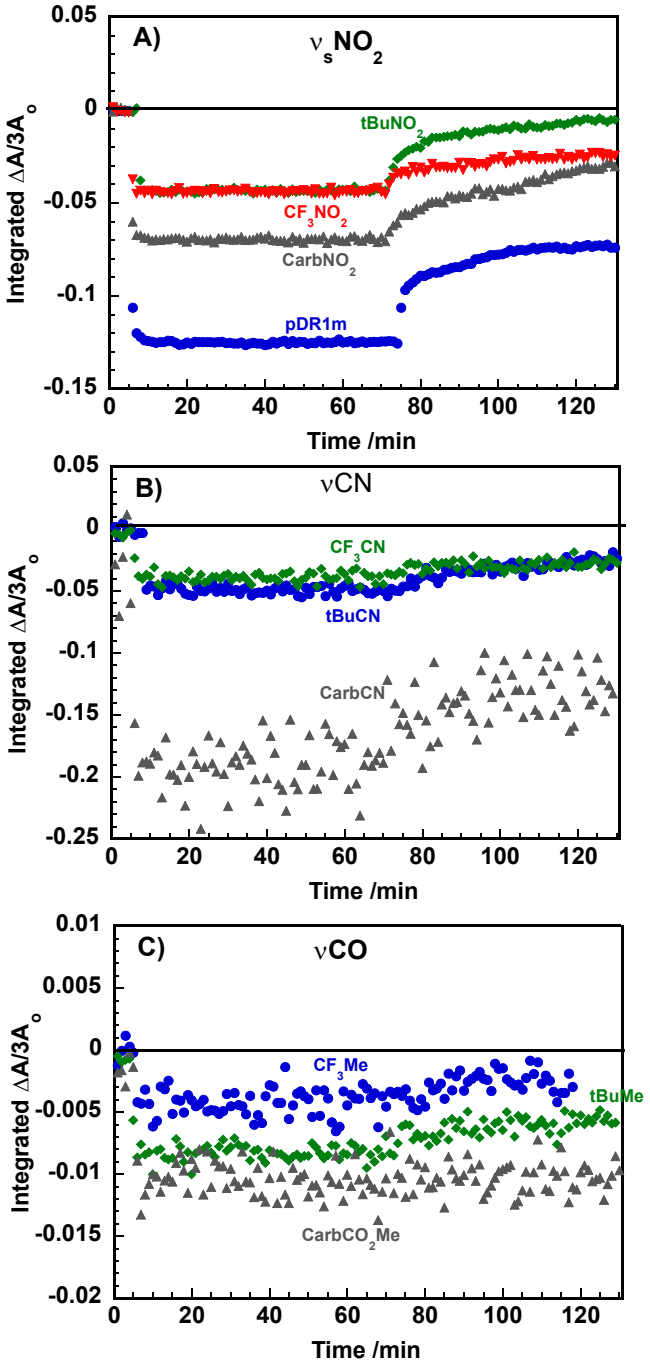

Figure 5. (A) Dynamics of orientation of the nitro symmetric stretching modes of **$tBuNO_2$**, **CF_3NO_2**, **$CarbNO_2$** and **pDR1M** thin films. (B) Dynamics of orientation of the CN symmetric stretching modes of **tBuCN**, **CF_3CN**, **CarbCN.**

Table 1. Summary of the properties of the azo polymer and triphenylaminoazo compounds processed as thin films on glass substrates. Fit parameters obtained from modeling the photoinduced birefringence curves in thin films recorded at a wavelength of 632.8 nm during an irradiation cycle (λ_{irr}= 532 nm, irradiance of 80 mW/cm^2). R is the correlation coefficient of the fit.

				Orientation cycle $y_{orientation}(t) = m_1^{or} e^{-k_1^{or} t} + m_2^{or} e^{-k_2^{or} t} + m_3^{or}$							
Compound	T_g °C	λ_{max}(abs) / nm	Film thickness / nm	m_1^{or}	k_1^{or} /s^{-1} **fast**	m_2^{or}	k_2^{or} /s^{-1} **slow**	m_3^{or} $\lvert\Delta n_{max}\rvert$	m_1^{or} **%**	m_2^{or} **%**	**R**
pDR1M-11%	110	492	470	-0.04619	1.337	-0.00435	0.0712	0.0458	91.4	8.6	0.993
tBuNO$_2$	118	508	450	-0.02437	7.641	-0.00044	0.0333	0.0252	98.2	1.8	0.992
tBuCN	117	482	580	-0.02796	9.400	-0.00063	0.0115	0.0283	97.8	2.2	0.995
tBuCO$_2$Me	112	468	520	-0.02100	5.229	-0.00128	0.0017	0.0206	94.5	5.5	0.941
CarbNO$_2$	202	508	480	-0.03214	2.535	-0.00171	0.0225	0.0317	94.9	5.1	0.990
CarbCN	201	482	375	-0.01455	5.550	-0.00494	0.5364	0.0198	74.7	25.3	0.992
CarbCO$_2$Me	187	468	550	-0.01898	1.712	-0.00104	0.0254	0.0198	94.8	5.2	0.986
CF$_3$NO$_2$	62	477	300	-0.01740	4.328	-0.00096	0.0079	0.0159	94.8	5.2	0.958
CF$_3$CN	68	457	450	-0.01602	8.450	-0.00037	0.1284	0.0162	97.7	2.3	0.983
CF$_3$CO$_2$Me	65	445	350	-0.01534	6.863	-0.00044	0.0884	0.0154	97.2	2.8	0.991

Table 2. Fit parameters obtained from modeling the birefringence relaxation curves recorded at a wavelength of 632.8 nm. R is the correlation coefficient of the fit.

	Relaxation cycle $y_{relaxation.}(t) = m_1^{rel}\left(1-e^{-k_1^{rel}t}\right) + m_2^{rel}\left(1-e^{-k_2^{rel}t}\right) + m_3^{rel}$							
Compound	m_1^{rel}	k_1^{rel} **/s^{-1} fast**	m_2^{rel}	k_2^{rel} **/s^{-1} slow**	$m_1^{rel}+m_2^{rel}+m_3^{rel}$ $\lvert\Delta n_{residual}\rvert$ (% residual birefringence)	**% (m_1)**	**% (m_2)**	**R**
pDR1M	-0.00558	0.276	-0.00650	0.015322	0.0316 (68.9%)	46.2	53.8	0.997
tBuNO$_2$	-0.00409	0.685	-0.01299	0.008517	0.0066 (26.2%)	24.0	76.0	0.999
tBuCN	-0.00206	0.132	-0.01359	0.005864	0.0092 (32.5%)	13.1	86.9	0.999
tBuCO$_2$Me	-0.00132	0.107	-0.00523	0.004600	0.0117 (56.7%)	20.1	79.9	0.998
CarbNO$_2$	-0.00173	0.070	-0.00772	0.007509	0.0215 (67.8%)	18.3	81.7	0.999
CarbCN	-0.00125	0.171	-0.00258	0.006020	0.0148 (74.7%)	32.7	67.3	0.996
CarbCO$_2$Me	-0.00071	0.146	-0.00221	0.004609	0.0161 (81.1%)	24.3	75.7	0.996
CF$_3$NO$_2$	-0.00172	0.131	-0.00757	0.007459	0.0049 (30.8%)	18.5	81.5	0.998
CF$_3$CN	-0.00369	0.187	-0.00724	0.005013	0.0059 (36.4%)	33.8	66.2	0.997
CF$_3$CO$_2$Me	-0.00183	0.263	-0.00260	0.009661	0.0098 (63.6%)	41.4	58.6	0.996

TOC Graphic

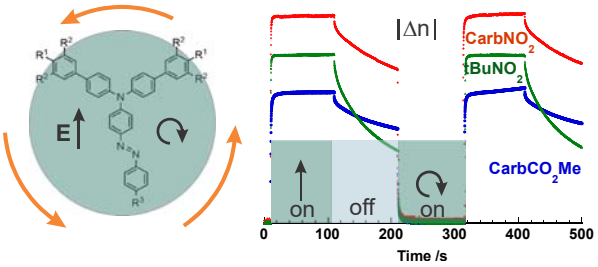
E
|Δn|
CarbNO2
tBuNO2
CarbCO2Me
on
off
on
0
100
200
300
400
500
Time /s